HHS Public Access

Author manuscript

Stem Cells. Author manuscript; available in PMC 2018 January 26.

Published in final edited form as:

Stem Cells. 2016 March ; 34(3): 601–613. doi:10.1002/stem.2298.

Comprehensive Proteomic Analysis of Mesenchymal Stem Cell Exosomes Reveals Modulation of Angiogenesis via Nuclear Factor-KappaB Signaling

Johnathon D. Anderson[a], **Henrik J. Johansson**[b], **Calvin S. Graham**[a], **Mattias Vesterlund**[b], **Missy T. Pham**[a], **Charles S. Bramlett**[a], **Elizabeth N. Montgomery**[a], **Matt S. Mellema**[c], **Renee L. Bardini**[a], **Zelenia Contreras**[a], **Madeline Hoon**[a], **Gerhard Bauer**[a], **Kyle D. Fink**[a], **Brian Fury**[a], **Kyle J. Hendrix**[a], **Frederic Chedin**[d], **Samir El-Andaloussi**[e,f], **Billie Hwang**[g], **Michael S. Mulligan**[g], **Janne Lehtiö**[b], and **Jan A. Nolta**[a]

[a]Stem Cell Program, Department of Internal Medicine, University of California Davis, Davis, California, USA

[b]Cancer Proteomics, Department of Oncology-Pathology, Karolinska Institutet, Stockholm, Sweden

[c]Surgical and Radiological Sciences, Department of Veterinary Medicine, University of California Davis, Davis, California, USA

[d]Department of Molecular and Cellular Biology, University of California Davis, Davis, California, USA

[e]Department of Laboratory Medicine, Karolinska Institutet, Stockholm, Sweden

[f]Department of Physiology, Anatomy and Genetics, University of Oxford, Oxford, United Kingdom

[g]Department of Surgery, University of Washington, Seattle, Washington, USA

Abstract

Mesenchymal stem cells (MSC) are known to facilitate healing of ischemic tissue related diseases through proangiogenic secretory proteins. Recent studies further show that MSC derived exosomes function as paracrine effectors of angiogenesis, however, the identity of which components of the

Correspondence: Johnathon D. Anderson, Ph.D., Institute for Regenerative Cures, University of California Davis Medical Center, 2921 Stockton Blvd, Room 1300, Sacramento, California 95817, USA. Telephone: (916)-703-9300; Fax: (916)-703-9310; joanderson@ucdavis.edu.

The copyright line for this article was changed on 18 March 2016 after original online publication

Author Contributions

J.D.A.: conception and design, financial support, collection and/or assembly of data, data analysis and interpretation, manuscript writing, and final approval of manuscript; H.J.J.: collection and/or assembly of data, data analysis and interpretation, manuscript writing, and final approval of manuscript; C.S.G.: manuscript writing and final approval of manuscript; M.V.: collection and/or assembly of data; M.T.P., C.S.B., and E.N.M.: collection and/or assembly of data and final approval of manuscript; R.L.B. and M.S.M.: collection and/or assembly of data, data analysis and interpretation, and final approval of manuscript; G.B.: conception and design, manuscript writing, and final approval of manuscript; K.D.F.: manuscript writing and final approval of manuscript; B.F.: conception and design, manuscript writing, and final approval of manuscript; F.C. and S.E.A.: conception and design, manuscript writing, and final approval of manuscript; J.L. and J.A.N.: financial support, manuscript writing, and final approval of manuscript.

Disclosure of Potential Conflicts of Interest

The authors indicate no potential conflicts of interest.

See www.StemCells.com for supporting information available online.

exosome proteome responsible for this effect remains elusive. To address this we used high-resolution isoelectric focusing coupled liquid chromatography tandem mass spectrometry, an unbiased high throughput proteomics approach to comprehensively characterize the proteinaceous contents of MSCs and MSC derived exosomes. We probed the proteome of MSCs and MSC derived exosomes from cells cultured under expansion conditions and under ischemic tissue simulated conditions to elucidate key angiogenic paracrine effectors present and potentially differentially expressed in these conditions. In total, 6,342 proteins were identified in MSCs and 1,927 proteins in MSC derived exosomes, representing to our knowledge the first time these proteomes have been probed comprehensively. Multilayered analyses identified several putative paracrine effectors of angiogenesis present in MSC exosomes and increased in expression in MSCs exposed to ischemic tissue-simulated conditions; these include platelet derived growth factor, epidermal growth factor, fibroblast growth factor, and most notably nuclear factor-kappaB (NFkB) signaling pathway proteins. NFkB signaling was identified as a key mediator of MSC exosome induced angiogenesis in endothelial cells by functional in vitro validation using a specific inhibitor. Collectively, the results of our proteomic analysis show that MSC derived exosomes contain a robust profile of angiogenic paracrine effectors, which have potential for the treatment of ischemic tissue-related diseases.

Keywords

Mesenchymal stem cells; Exosomes; Proteomics; Peripheral arterial disease; Nuclear factor kappaB; High-resolution isoelectric focusing; Liquid chromatography tandem mass spectrometry

Introduction

Ischemic tissue related diseases such as peripheral arterial disease (PAD) affect 8–12 million people every year in the US, and often there are no satisfactory treatment options for many of these patients. PAD is characterized by a lack of proper blood flow to the lower extremities due to narrowing or blockage of arterial vasculature from atherosclerotic plaques [1]. Angioplasty and stent placement are commonly used to treat PAD, however, restenosis and reocclusion from subsequent blood clot formation and stent overgrowth limit the effectiveness of these treatments in many patients [2, 3]. A potential alternative therapeutic approach is localized induction of angiogenesis to restore blood flow to affected tissues. Several studies in animal models of PAD have shown localized induction of angiogenesis via recombinant Vascular endothelial growth factor (VEGF) therapy to be beneficial. However, this straightforward approach has so far failed to show clear benefits in humans in late-stage clinical trials, perhaps due to the use of a monotherapeutic approach which only targeted a single signaling pathway responsible for only one portion of the tissue healing process in PAD [4].

Bone marrow derived mesenchymal stem cells (MSCs) exhibit tissue healing capabilities via signaling to endogenous cell populations including immune cells and endothelial cells [5]. MSCs have also shown promise as a potential therapeutic for PAD through the secretion of a robust profile of angiogenic signaling proteins, however, it remains unclear which factors are the main drivers of MSC induced angiogenesis [6]. Exosomes are small lipid-bound,

cellularly secreted vesicles that mediate intercellular communication via cell-to-cell transport of proteins and RNA [7]. Interestingly, exosomes have been recently shown to also mediate some of the tissue healing properties of MSCs [8–10], however, the underlying mechanisms by which MSC derived exosomes exert their tissue healing properties remain unclear.

Additionally, the angiogenic potential of MSCs can vary due to differences in their microenvironment [11]. MSCs are generally expanded in high serum (10%–20%) containing media under atmospheric oxygen (normoxic) conditions (21% O_2) prior to injection into animal models [12]. However, MSCs experience a markedly different environmental niche upon injection into tissues affected by PAD, where they are exposed to significantly reduced oxygen tension and a reduced concentration of factors contained in serum due to a lack of proper blood flow [13]. It has been recognized that the angiogenic potential of endothelial cells is enhanced when stimulated under hypoxic conditions [14]. Although there is evidence that hypoxic stimulation induces expression of angiogenic signaling proteins in endothelial cells, it is not clear to what extent such changes in the environmental niche affect the MSC proteome [15, 16]. Therefore, we characterized signaling pathways and gene networks that are differentially expressed at the protein level in MSCs exposed to PAD-like culture conditions as compared to normoxic, high serum expansion conditions.

As proteins mediate most intracellular activity and communication between cells, mass spectrometry proteomics approaches have been invaluable in elucidating differential cell states and patterns of cellular communication [17]. However, mass spectrometry-based proteomics approaches have had limitations in depth of analysis, greatly limiting the characterization of signaling proteins within cells as they are often present at low levels as compared to other classes of proteins such as structural proteins, which are present at much higher levels [18]. Recently we developed a new mass spectrometry approach termed high-resolution isoelectric focusing liquid coupled chromatography tandem mass spectrometry (HiRIEF LC-MS/MS) that enable deep proteome coverage of cellular lysates [19]. This approach has been demonstrated by Branca et al. to be capable of quantitatively characterizing >10,000 proteins per cell lysate, whereas other methods of mass spectrometry generate datasets with smaller depth of coverage [19].

Here we focus on investigating the effects of a PAD-like microenvironment on angiogenic signaling protein expression within MSCs and their secreted exosomes. We use HiRIEF LC-MS/MS to investigate changes in MSC proteomic expression when cultured under normoxic, high serum expansion conditions as compared to conditions that mimic the microenvironment experienced by MSCs upon injection into tissues affected by PAD. We find that exposure of MSCs to a PAD-like microenvironment increases expression of several proangiogenic signaling associated proteins including epithelial growth factor (EGF), fibroblast growth factor (FGF), and platelet derived growth factor (PDGF). In addition, we find that exposure of MSCs to a PAD-like microenvironment induces elevated exosome secretion and that these secreted exosomes contain a robust angiogenic signaling profile and are capable of inducing angiogenesis in vitro via the nuclear factor kappa-light-chain enhancer of activated B-cells (NFkB) pathway.

Materials and Methods

Cell Culture and Reagents

Human bone marrow aspirates from young adult, nonsmoking males were obtained from Lonza (Allendale, NJ, http://www.lonza.com). For MSC isolation and expansion, bone marrow aspirates were passed through 90 μm pore strainers for isolation of bone spicules. Then, the strained bone marrow aspirates were diluted with equal volume of phosphate-buffered saline (PBS) and centrifuged over Ficoll (GE Healthcare, Waukesha, WI, http://www.ge-healthcare.com) for 30 minutes at 700*g*. Next, mononuclear cells and bone spicules were plated in plastic culture flasks, using minimum essential media α (MEM-α) (HyClone Thermo Scientific, Waltham, MA, http://www.hyclone.com) supplemented with 10% fetal bovine serum (FBS; Atlanta Biologicals, Lawrenceville, GA, http://www.atlantabio.com) that had been screened for optimal MSC growth. After 2 days, nonadherent cells were removed by two to three washing steps with PBS. After passage 2 MSCs were expanded in 20% FBS and MSCs from passages 5–6 were used for experimentation. For serum starvation studies MSCs were washed three times with PBS and cultured in exosome isolation media consisting of OptiMEM without phenol red with 1% L-Glut (IC) (Life Technologies, Carlsbad, CA, http://www.lifetechnologies.com) for 40 hours. For serum starvation plus low oxygen conditions (PAD) MSC were cultured in exosome isolation media under 1% oxygen tension for 40 hours. Pooled human human umbilical cord vein endothelial cells (HUVECs) were purchased from Lonza and cultured according to manufacturer's instructions using EndoGRO-LS Complete media from Millipore (Billerica, MA, http://www.emdmillipore.com).

Vesicle Isolation and Characterization

MSC were washed three times with PBS and switched to exosome isolation media; either 20% FBS media that was pre-cleared of exosomes via 18 hour 120,000*g* centrifugation or OptiMEM (Life Technologies) and were conditioned for 40 hours prior to vesicle isolation [9]. Microvesicles (MV) were isolated as in previous studies [20]. Briefly conditioned media was cleared of cells and cell debris via centrifugation (500*g* and 1,000*g*, respectively), then spun at 17,000*g* pellet to isolate MVs. Exosomes were isolated as in previous studies [20]. Briefly, for proteomics studies exosomes were isolated using 0.22 μm filtration to get rid of cells, cell debris and MVs prior to being spun at 120,000*g* for 2 hours, the pellet was then washed with 39 mL of PBS and spun again at 120,000*g* for 2 hours. All ultracentrifuge steps were performed with a Ti70 rotor in polyallomer quick seal tubes (Beckman Coulter, Brea, CA http://www.beckmancoulter.com). Vesicle concentration was determined using detergent compatible protein concentration (DC) assay (BioRad, Hercules, CA, http://www.bio-rad.com), and size distribution was assessed using NanoSight LM10HS (Malvern, Amesbury, MA, http://www.malvern.com).

Electron Microscopy

Scanning electron microscopy (SEM) images were taken with Philips XL30 TMP (FEI Company, Hillsboro, OR, http://www.fei.com). Sputter Coater: Pelco Auto Sputter Coater SC-7, (Ted Pella, Redding, CA, http://www.tepella.com). Transmission electron microscopy (TEM) images were taken on Philips CM120 Biotwin Lens, 9 (FEI Company), with 2%

uranyl acetate staining using facilities at Electron Microscopy Laboratory, School of Medicine, University of California at Davis.

Sample Preparation for Proteomics

Cell pellets were lysed with 4% SDS, 25 mM HEPES, 1 mM dithiothreitol (DTT). EVs were lysed with 2% SDS, 25 mM HEPES, 1 mM DTT. Lysates were heated to 95°C for 5 minutes followed by sonication for 1 minute, and centrifugation 14,000*g* for 15 minutes. The supernatant was mixed with 1 mM DTT, 8 M urea, 25 mM HEPES, pH 7.6, transferred to a centrifugation filtering unit, 10 kDa cutoff (Nanosep, Pall, Port Washington, NY, http://www.pall.com), and centrifuged for 15 minutes, 14,000*g*, followed by another addition of the 8 M urea buffer and centrifugation. Proteins were alkylated by 50 mM indoleacetic acid (IAA), in 8 M urea, 25 mM HEPES for 10 minutes, centrifuged for 15 minutes, 14,000*g*, followed by two more additions and centrifugations with 8 M urea, 25 mM HEPES. Trypsin (Promega, Madison WI, http://www.promega.com), 1:50, trypsin:protein, was added to the cell lysate in 250 mM urea, 50 mM HEPES, and incubated overnight at 37°C. The filter units were centrifuged for 15 minutes, 14,000*g*, followed by another centrifugation with MQ, and the flow-through was collected [19]. Peptides from EVs were TMT6 labeled and MSC cells with TMT10 labeled according to manufacturer's instructions (Thermo Fisher Scientific, San Jose, CA, http://www.thermofisher.com). Peptides were cleaned by a strata-X-C-cartridge (Phenomenex, Torrance, CA, http://www.phenomenex.com) [19, 21].

Proteomics on nLC-MS/MS on Thermo Scientific LTQ Orbitrap Velos

Before analysis of exosomes on LTQ-Orbitrap Velos (Thermo Fischer Scientific), peptides were separated using an Agilent 1200 nano-LC system. Samples were trapped on a Zorbax 300SB-C18 and separated on a NTCC-360/100-5-153 (Nikkyo Technos, Tokyo, Japan, http://www.nikkyo-tec.co.jp) column using a gradient of A (5% Dimethyl sulfoxide (DMSO), 0.1% formic acid (FA)) and B (90% acetonitrile (ACN), 5% DMSO, 0.1% FA), ranging from 3% to 40% B in 45 minutes with a flow of 0.4 μL/minute. The LTQ-Orbitrap Velos was operated in a data-dependent manner, selecting five precursors for sequential fragmentation by collision-induced dissociation (CID) and higher-energy C-trap dissociation (HCD) and analyzed by the linear iontrap and orbitrap, respectively. The survey scan was performed in the Orbitrap at 30,000 resolution (profile mode) from 300 to 2,000 m/z with a max injection time of 500 millisecond and automatic gain control (AGC) set to 1×10^6 ions. For generation of HCD fragmentation spectra, a max ion injection time of 500 milliseconds and AGC of 5×10^4 were used before fragmentation at 37.5% normalized collision energy. For fourier transform mass spectrometry (FTMS) mass spec 2 (MS2) spectra, normal mass range was used, centroiding the data at 7,500 resolution. Peptides for CID were accumulated for a max ion injection time of 200 milliseconds and AGC of 3×10^4, fragmented with 35% collision energy, wideband activation on, activation q 0.25, activation time 10 milliseconds before analysis at normal scan rate and mass range in the linear iontrap. Precursors were isolated with a width of 2 m/z and put on the exclusion list for 60 seconds. Single and unassigned charge states were rejected from precursor selection.

Proteomic Data Analysis

GraphPAD Prism was used to calculate differential expression using multiple *t* tests and a stringent false discovery cut off of 1% (GraphPAD Prism, La Jolla, CA, http://www.graphpad.com). Panther Pathway analysis was used to detect the number of pathways detected in each sample and the number of proteins of each pathway represented in each sample (http://www.pantherdb.com). Ingenuity pathway analysis (IPA) software was used to analyze enrichment for signaling pathway proteins and putative functionality of proteins present in and between each sample (Qiagen, Redwood City, CA, http://www.ingenuity.com). ClueGO software was used for gene ontology (GO) analysis of each sample to detect broad classes of protein functionality (http://www.ici.upmc.fr/cluego/cluegoDownload.shtml). CytoScape was used to generate network interactome maps for the angiogenesis interactome of MSCs and exosomes and the NFkB pathway interactome (http://www.cytoscape.org). The constructed angiome dataset from Chu et al. was used to search for the presence of canonical angiogenesis mediating proteins in our data, with the addition of physically interacting proteins not found in the Chu et al. dataset. The Spike database was used to detect proteins for which there was experimental evidence for physical interactions (i.e., yeast-2-hybrid, coimmunoprecipitation) with the Chu et al. dataset and was accessed via CytoScape.

Tubule Formation Migration Assay

Primary HUVECs were purchased from Lonza and cultured in EndoGRO-LS Complete (Millipore) media as per manufacturer's protocol and plated on growth factor reduced Matrigel (Corning, Corning, NY, http://www.corning.com) and stained with Calcein AM (Life Technologies) and imaged at 16 hours poststimulation at × 4 on a Kenyence BZ-9000F (Keyence, Osaka, Japan, http://www.keyence.com). EndoGRO basal media was used for control and exosome stimulated wells and EndoGRO-LS Complete was used as a positive control (Millipore). For NFkB inhibitor experiments pyrrolidine dithiocarbamate (PDTC) was used at a concentration of 50 μM.

Results

MSCs Exposed to PAD-Like Conditions Show Dynamic Proteomic Changes

To address what effect PAD-like microenvironment conditions have on the proteomic profile of MSCs, HiRIEF LC/MS-MS was used to quantify the proteome of MSCs. Human MSCs derived from the bone marrow of three young adult, nonsmoking male donors were cultured under normoxic, high serum expansion conditions until passage 6. After three PBS washes, MSCs were cultured under one of three culture conditions for 40 hours: normoxic, high serum expansion conditions (EX: 20% FBS, 21% O_2), PAD-like conditions (PAD: 0% FBS, 1% O_2), or an intermediate condition (IC: 0% FBS, 21% O_2) (Fig. 1A).

A total of 6,342 proteins were identified and quantified in each of the nine MSC samples, with three donors for each of the three conditions (Supporting Information Table S1). A total of 580 membrane associated proteins were detected in each of the nine MSC samples, including canonical MSC surface markers: CD73 (NT5E), CD90 (THY1), and CD105 (ENG) (Supporting Information Fig. S1; Tables S2, S3). Our data overlaps with and expands

beyond the work by Mindaye et al. Statistical analysis of protein expression levels using a false discovery rate of 1% (FDR1%) revealed 315 and 843 differentially expressed proteins, respectively between the EX versus IC and EX versus PAD conditions (Supporting Information Tables S4, S5). Analysis of MSC differential expression ratios versus abundance (area) revealed differentially expressed proteins were distributed across the range of abundances of all cellular proteins (Fig. 1). This indicated that the effects of the culture conditions on protein expression were not limited to lowly expressed proteins. Analysis of MSC differential expression ratios versus *p* value demonstrated that significantly differentially expressed proteins (FDR1%) were distributed across the range of ratios for all cellular proteins. This indicated that the effects of the culture conditions on protein expression included many new and highly significant findings (Fig. 1).

Although global heatmap cluster analysis and linear regression analysis of PAD/EX ratios revealed donor to donor variation in MSCs, it also revealed robust intracondition concordance between donors (Fig. 2, Supporting Information Fig. S2), especially of significantly differentially expressed proteins. MSCs exposed to PAD-like conditions showed significant increases (FDR1%) in rate limiting proteins of glycolysis (ALDOB, ENO3, and PGK1) and the NRF2/glutathione pathway (ASK1, MKK3/6, and FTH1), which are metabolic and antioxidant associated pathways that have been shown to be modulated with exposure to lower oxygen tension (Fig. 1; Supporting Information Figs. S3, S4) [22, 23]. IC-conditioned MSCs, in contrast, showed no such increases (FDR1%) in glycolysis and glutathione related pathway proteins as compared to the EX condition. GO analysis using Cytoscape's ClueGO plugin of significantly differentially expressed proteins (FDR1%) revealed numerous cell cycle checkpoint-related pathways (G1 phase, G2/M phase, and cytokinesis) involved in the regulation of cellular proliferation were downregulated in both IC and PAD conditions as compared to the EX condition (Supporting Information Figs. S5–S9). Cholesterol and lipid biosynthesis pathways were upregulated in both IC and PAD conditions as compared to the EX condition (Fig. 2; Supporting Information Figs. S10, S11) [24].

Exposure of MSCs to a PAD-like environment induced significant changes in their proteome. Previous studies have indicated that MSCs are capable of inducing angiogenesis, therefore, we analyzed how this PAD-like microenvironment modulated levels of their angiogenic signaling proteins [25–27]. To investigate the interaction patterns of known angiogenic proteins in MSCs and to elucidate proteins that physically interact with these known angiogenic proteins, we developed an angiogenesis interactome network map of the MSC proteome. To generate the angiogenesis interactome network map we derived a list of known angiogenic proteins from Chu et al. that were shown to be present in the MSC proteome [28]. We then used CytoScape to include proteins that had experimental evidence of physical interaction with these MSC exosome angiogenic proteins and to show how they interacted with each other [29]. The advantage of this approach is that it not only elucidates the physical interactions of canonical angiogenesis proteins but also additionally reveals other noncanonical proteins that physically interact with the angiome, thereby shedding light on potentially novel mediators of angiogenesis. Analysis of the angiogenesis interactome of proteins present in MSCs across all three donors exposed to each of the three conditions revealed the most robust clustering of signaling protein interactions was with platelet derived

growth factor receptor (PDGFR), epidermal growth factor receptor (EGFR), and NFkB nodes (Supporting Information Figs. S12–S14). This indicates that these pathways are likely drivers of MSCs' proangiogenic potential. Furthermore, using Panther pathway analysis, we found several angiogenic pathways to be significantly (FDR1%) upregulated in MSCs exposed to PAD-like conditions, including canonical angiogenic associated pathways of PDGF, EGF, and FGF (Fig. 2) [30]. These data collectively demonstrate significantly increased expression of several angiogenic signaling pathways and cholesterol/lipid biosynthesis pathways in MSCs exposed to the PAD condition as compared to the conventional EX condition.

MSC Exosome Secretion Increases Under PAD-Like Conditions

Newly synthesized membrane components such as lipids and cholesterol are transported from their site of genesis at the endoplasmic reticulum to the plasma membrane via vesicular transport [31, 32]. However, as cells experience decreased rates of proliferation their need for newly synthesized plasma membrane components should also decrease [33]. We observed that a variety of cell cycle pathways decreased in expression in the IC and PAD conditions as expected, since the cells were exposed to a lower oxygen tension and deprived of growth factor stimulation. Interestingly however, we observed that cholesterol/lipid biosynthesis proteins actually significantly (FDR1%) increased in expression and not decreased, in both IC and PAD conditions as compared to the expansion condition, EX (Supporting Information Figs. S10, S11). This led us to speculate that perhaps an increase in exosome biogenesis could account for the increased expression of proteins involved in cholesterol/lipid biosynthesis. Indeed we observed a trend towards increased expression of proteins involved in the biogenesis of exosomes, prompting us to analyze vesicle secretion of MSCs (Supporting Information Fig. S15).

Extracellular vesicles secreted from MSCs (MVs, exosomes) were isolated from media that had been conditioned for 40 hours under EX, IC, and PAD culture conditions using ultracentrifugation. Analysis of vesicle yield via BCA protein concentration assays revealed that MSC MV secretion decreased whereas exosome secretion substantially increased with MSCs exposed to IC and PAD conditions as compared to EX conditions (Fig. 3). However, exosomes isolated from the EX condition coisolated with FBS protein from the media (Supporting Information Fig. S16). SEM images of MSCs exposed to PAD conditions showed vesicle structures consistent with a decrease in microvesicle secretion and an increase of exosome secretion as compared to MSC exposed to EX conditions (Fig. 3). Furthermore, TEM of isolated PAD-derived MSC exosomes with negative staining is consistent with canonical exosome morphology; additionally, Nanosight analysis revealed that MSC exosomes were of expected size range and MSCs maintained low levels of apoptosis in all conditions (Fig. 3; Supporting Information Fig. S16).

MSC Exosome Proteome Contains a Robust Profile of Angiogenic Signaling Proteins

As two recent studies demonstrated that MSC exosomes are proangiogenic both in vitro and in vivo, we used MSC HiRIEF LC-MS/MS to characterize the proteome of MSC derived exosomes from MSCs exposed to IC and PAD conditions [8, 34]. A total of 1,927 proteins were quantified in each of the six samples generated from cells derived from three donors

under both the PAD and IC conditions (Supporting Information Table S1), 457 of which were not detected in MSCs, indicating exosomal enrichment (Supporting Information Table S6). We detected 92 of the top 100 most identified exosomal marker proteins from the ExoCarta database in each of our exosome samples from both conditions, IC and PAD (Supporting Information Table S7; Supporting Information Fig. S16) [35–37]. Differential expression analysis of exosomes from IC and PAD conditions revealed few significant expression differences (FDR1%) in exosomes between IC and PAD conditions (Supporting Information Table S8).

GO analysis using Cytoscape's ClueGO plugin of the MSC exosome proteome from all three donors from both conditions showed representation of vascular and endothelial associated proteins (Fig. 4) [38]. GO analyses are generally broad based and helpful for a broad overview of the data but are generally limited in their ability to identify specific signaling pathways. We therefore performed Panther pathway analysis on the MSC exosome proteome and found high representation of several canonical angiogenic associated pathways: cadherin, EGFR, FGF, and PDGF (Fig. 4).

IPA is a robust high throughput data analysis software that is able to predict the induction or inhibition of various cellular activities based on an expert, manually curated database of known protein associations and functions. IPA analysis showed that MSC exosomes contain numerous proteins with a variety of angiogenesis-related functionalities including induction of: angiogenesis, vasculogenesis, cell migration, and endothelial cell proliferation (Supporting Information Figs. S17–S20).

Next we performed network analysis of the angiogenesis interactome of MSC exosomes, as with the MSC proteome. We showed the most robust representation of protein nodes clustered around the canonical angiogenic pathways of NFKB1/2, Avian Reticuloendotheliosis Viral Oncogene Homolog A (RELA), PDGFRB, and EGFR in our angiogenesis interactome network map (Fig. 5). Furthermore, network analysis of the NFkB pathway showed robust representation of MSC exosome proteins clustering around RELA, NFKB1/2, and TNF-receptor associated factor 6 (Supporting Information Fig. S21). These data collectively showed that exosomes derived from MSCs exposed to PAD-like conditions contain a robust profile of angiogenic signaling proteins and putative functionalities closely mirroring those found in MSCs.

MSC Exosomes Induce Angiogenesis via the NFkB Pathway in Endothelial Cells

To test the angiogenic potential of MSC exosomes, HUVECs were stimulated in vitro with PAD-derived MSC exosomes. To evaluate their ability to induce tubule formation, a canonical in vitro assay of angiogenesis was applied. Traditionally, putative therapeutics are known to have a therapeutic index where they behave in a dose dependent manner with decreased effectiveness generally observed at higher doses [39]. HUVECs were treated with increasing doses of PAD-derived MSC exosomes to test for their effective dose range. The low dose of PAD-derived MSC exosomes (1 μg/mL) induced significant tubule formation compared to the unstimulated control, as did the medium dose (10 μg/mL), measured by total segment length (Fig. 6). However, the high dose of PAD-derived MSC exosomes (100

μg/mL) was less effective than the medium dose indicating the upper limits of the effective dose range (Fig. 6).

In our network analysis map of the MSC exosome angiogenesis interactome, we observed several hubs of clustering around nodes of the NFkB complex, which is known to mediate angiogenic signaling. Even though these particular nodes, which represent core components of the NFkB complex, were not detected in the MSC exosomes we hypothesized that the presence of numerous NFkB interacting proteins may indicate a potential effector role of this pathway in HUVEC tubule formation. To test this hypothesis HUVECs were treated with PDTC, a specific inhibitor of NFkB signaling or vehicle control prior to stimulation with PAD-derived MSC exosomes in a tubule formation assay. PAD-derived MSC exosomes induced tubule formation in HUVECs treated with the vehicle control but not in HUVECs treated with PDTC, demonstrating that NFkB signaling is necessary for MSC exosome induction of tubule formation in vitro (Fig. 7). These results indicate that MSC exosomes mediate angiogenesis in a dose dependent manner via the NFkB pathway.

Discussion

This study presents, to our knowledge, the most robust proteomic characterization of MSCs and exosomes to date (MSC = 6,342 vs. 1,024, MSC exosome = 1,927 vs. 236) [40, 41]. We detected 580 membrane associated proteins including those required to meet the minimal criteria for MSC classification (CD73, CD90, CD105) across all nine MSC samples and represents the most robust proteomic profiling of MSC membrane proteins to date (580 vs. 172) [42]. MSCs have been proposed as a therapeutic for PAD, however, the effect of the PAD microenvironment has on both the MSC physiology and MSC induced angiogenesis are poorly understood [43]. Even though several studies have demonstrated the efficacy of using MSCs for ischemic tissue related diseases, efforts toward identifying the underlying mechanisms of MSC induced angiogenesis have not been robustly investigated, as more focus has been placed on MSC secretion of VEGF and PDGF [44–47]. The quantitative proteomic methodology we used underscores the need for an unbiased approach which in the present study led to the finding that the MSC proteome is modulated upon exposure to a PAD-like microenvironment and multiple pathways are likely involved in MSC mediated angiogenesis.

We show attenuation of various cell cycle initiation and glycolysis gene networks in MSCs exposed to PAD-like conditions. Network analysis of all three donors from all three culture conditions (nine samples total) demonstrated that the MSC angiogenesis interactome is enriched for nodes associated with PDGFR, EGFR, and NFkB. This indicated that these known angiogenesis mediating pathways are likely central hubs of intracellular angiogenic signaling within MSCs [48–51]. Furthermore, when MSCs were exposed to PAD-like conditions they significantly increased expression of proteins associated with a subset of angiogenic signaling pathways EGF, FGF, and PDGF.

MSCs are known to mediate much of their tissue healing effects through their secretome in various vascular disease models such as stroke and peripheral arterial disease [5, 52]. Recent studies have demonstrated that a new cell to cell communication system mediated by

exosomes is capable of recapitulating much of the beneficial therapeutic effects of MSCs in these disease models [8–10, 53]. However, the underlying mechanisms by which MSC exosomes modulate these tissue healing effects have yet to be elucidated.

We characterized the proteome of exosomes derived from MSCs exposed to PAD-like conditions (PAD) and the IC, but not from EX since our HiRIEF LC-MS/MS method requires large quantities of input material and the exosome yield from this condition was too small. We quantitatively characterized 1,927 proteins in MSC exosomes from all three donors across both IC and PAD conditions, of which 457 were not detected in the MSC proteome. A potential explanation for this observed protein enrichment in MSC exosomes is that some proteins can be masked in more complex lysates when using mass spectrometry methodologies, but this does not preclude the possibility that some of these proteins are being directly shuttled into exosomes for secretion [18]. Of note is the fact that the proteome of exosomes derived from MSCs appears to lack many canonical secretory signaling proteins such as cytokines and growth factors, but instead contain the downstream mediators of these pathways.

We showed that exosomes from MSCs exposed to PAD-like conditions contain a robust profile of angiogenesis associated proteins that closely mirror the upregulated angiogenic pathways found in MSCs exposed to PAD-like conditions including EGFR, FGF, and PDGF pathways. These findings suggest that upon exposure to ischemic tissue conditions attempt to generate a more proangiogenic state via the secretion of exosomes, thereby facilitating localized tissue healing. An interesting unresolved question worthy of further exploration is whether the main drivers of MSC exosome induced angiogenesis act via direct signaling to endothelial cell populations or indirectly through inducing chemotaxis of immune cells such as monocytes.

We also showed that proteins mediating cholesterol/lipid biosynthesis and metabolism are significantly upregulated in MSCs that are exposed to PAD-like conditions, while several known exosome biogenesis proteins trend toward increased expression under these same conditions. Numerous cell cycle pathways are significantly downregulated in MSCs exposed to PAD-like conditions and various cell types have substantially lower rates of proliferation when exposed to similar conditions [11, 16]. Since, ostensibly there should be much less demand for such high energy cost membrane components and exosomes are known to be enriched for lipid raft components such as cholesterol [54], we therefore speculated that the upregulation of these cholesterol/lipid biosynthesis proteins may be associated with exosome secretion. We showed that MSCs increased secretion of exosomes upon exposure to PAD-like conditions which were of canonical size and morphology. Alternatively the observed increase in lipid biosynthesis may potentially be a cellular adaption to hypoxia in the PAD condition [55].

Consistent with traditional broad range small molecule dose curves, we show that exosomes derived from MSCs exposed to PAD-like conditions were able to induce angiogenesis in vitro, in a dose dependent manner. MSC exosomes at the highest concentration (100 μg/mL) induced less tubule formation as compared to lower doses, which may indicate an upper limit of the effective dosing range.

Our network analysis indicated that MSC exosomes derived from PAD-like conditions are enriched for several nodes associated with NFkB signaling, which has previously been shown to be an important mediator of angiogenesis [51]. We demonstrated that MSC exosome induced angiogenesis is dependent on NFkB signaling, since a specific chemical inhibitor of NFkB signaling completely abrogates the ability of MSC exosomes to induce tubule formation in vitro. It remains unclear, however, to what extent MSC induced angiogenesis can be attributed to exosome mediated effects. Overall, our data suggest that there are more signaling pathways involved which are worthy of further investigation.

Conclusion

A common trend that is becoming apparent across the MSC exosome literature is that exosomes derived from MSCs are able to mediate much of the functionality traditionally associated with canonical secretory proteins such as growth factors of the MSC secretome [8–10, 34, 56–60]. Whether canonical secretory proteins or exosomally delivered proteins are the main drivers of the MSC secretome's functionality still needs further investigation; based on our data it is likely microenvironment dependent.

An exciting open question is whether MSC exosomes derived from PAD-like culture conditions can be used as a therapeutic in lieu of MSCs for a various diseases and if so what the underlying therapeutic mechanisms might be. A study published in 2014 on the first human patient successfully treated with MSC exosomes for graft versus host disease would seem to suggest that this area of research is feasible and worthy of further investigation [9]. Our preliminary data suggest that MSC derived exosomes may be a promising therapeutic platform that provides additional benefits to the use of MSCs themselves. Our data may also provide a blueprint for future studies aiming to attempt to engineer MSC exosomes to be a more efficacious therapeutic for cardiovascular diseases.

Supplementary Material

Refer to Web version on PubMed Central for supplementary material.

Acknowledgments

This research was supported by funding provided by NIH Transformative R01GM099688, NSF GROW 201111600, NIH T32-GM008799, NIH T32 HL086350 and NSF GRFP 2011116000, SELA is supported by the Swedish Research Council (VR-Med and EuroNanoMedII).

References

1. Milani RV, Lavie CJ. The role of exercise training in peripheral arterial disease. Vasc Med. 2007; 12:351–358. [PubMed: 18048473]
2. Katz G, Harchandani B, Shah B. Drug-eluting stents: The past, present, and future. Curr Atherosclerosis Rep. 2015; 17:485.
3. Banfi A, von Degenfeld G, Gianni-Barrera R, et al. Therapeutic angiogenesis due to balanced single-vector delivery of VEGF and PDGF-BB. FASEB J. 2012; 26:2486–2497. [PubMed: 22391130]

4. Yla-Herttuala S, Rissanen TT, Vajanto I, et al. Vascular endothelial growth factors: Biology and current status of clinical applications in cardiovascular medicine. J Am Coll Cardiol. 2007; 49:1015–1026. [PubMed: 17349880]
5. Meyerrose T, Olson S, Pontow S, et al. Mesenchymal stem cells for the sustained in vivo delivery of bioactive factors. Adv Drug Deliv Rev. 2010; 62:1167–1174. [PubMed: 20920540]
6. Liew A, O'Brien T. Therapeutic potential for mesenchymal stem cell transplantation in critical limb ischemia. Stem Cell Res Ther. 2012; 3:28. [PubMed: 22846185]
7. S ELA, Mager I, Breakefield XO, Wood MJ. Extracellular vesicles: Biology and emerging therapeutic opportunities. Nat Rev Drug Discov. 2013; 12:347–357. [PubMed: 23584393]
8. Bian S, Zhang L, Duan L, et al. Extracellular vesicles derived from human bone marrow mesenchymal stem cells promote angiogenesis in a rat myocardial infarction model. J Mol Med. 2014; 92:387–397. [PubMed: 24337504]
9. Kordelas L, Rebmann V, Ludwig AK, et al. MSC-derived exosomes: A novel tool to treat therapy-refractory graft-versus-host disease. Leukemia. 2014; 28:970–973. [PubMed: 24445866]
10. Zhang B, Wang M, Gong A, et al. HucMSC-exosome mediated-Wnt4 signaling is required for cutaneous wound healing. Stem Cells. 2015; 33:2158–2168. [PubMed: 24964196]
11. Rosova I, Dao M, Capoccia B, et al. Hypoxic preconditioning results in increased motility and improved therapeutic potential of human mesenchymal stem cells. Stem Cells. 2008; 26:2173–2182. [PubMed: 18511601]
12. Ikebe C, Suzuki K. Mesenchymal stem cells for regenerative therapy: Optimization of cell preparation protocols. BioMed Res Int. 2014; 2014:951512. [PubMed: 24511552]
13. Banfi A, von Degenfeld G, Blau HM. Critical role of microenvironmental factors in angiogenesis. Curr Atheroscler Rep. 2005; 7:227–234. [PubMed: 15811258]
14. Humar R, Kiefer FN, Berns H, et al. Hypoxia enhances vascular cell proliferation and angiogenesis in vitro via rapamycin (mTOR)-dependent signaling. FASEB J. 2002; 16:771–780. [PubMed: 12039858]
15. Yamakawa M, Liu LX, Date T, et al. Hypoxia-inducible factor-1 mediates activation of cultured vascular endothelial cells by inducing g multiple angiogenic factors. Circ Res. 2003; 93:664–673. [PubMed: 12958144]
16. Beegle J, Lakatos K, Kalomoiris S, et al. Hypoxic preconditioning of mesenchymal stromal cells induces metabolic changes, enhances survival and promotes cell retention in vivo. STEM CELLS. 2015
17. Johansson HJ, Sanchez BC, Mundt F, et al. Retinoic acid receptor alpha is associated with tamoxifen resistance in breast cancer. Nat Commun. 2013; 4:2175. [PubMed: 23868472]
18. Hultin-Rosenberg L, Forshed J, Branca RM, et al. Defining, comparing, and improving iTRAQ quantification in mass spectrometry proteomics data. Mol Cell Proteomics. 2013; 12:2021–2031. [PubMed: 23471484]
19. Branca RM, Orre LM, Johansson HJ, et al. HiRIEF LC-MS enables deep proteome coverage and unbiased proteogenomics. Nat Methods. 2014; 11:59–62. [PubMed: 24240322]
20. Witwer KW, Buzas EI, Bemis LT, et al. Standardization of sample collection, isolation and analysis methods in extracellular vesicle research. J Extracell Vesicles. 2013; 2
21. Wisniewski JR, Zougman A, Nagaraj N, et al. Universal sample preparation method for proteome analysis. Nat Methods. 2009; 6:359–362. [PubMed: 19377485]
22. Lai JC, Behar KL. Glycolysis-citric acid cycle interrelation: A new approach and some insights in cellular and subcellular compartmentation. Dev Neurosci. 1993; 15:181–193. [PubMed: 7805570]
23. Hayes JD, Dinkova-Kostova AT. The Nrf2 regulatory network provides an interface between redox and intermediary metabolism. Trends Biochem Sci. 2014; 39:199–218. [PubMed: 24647116]
24. Saito R, Smoot ME, Ono K, et al. A travel guide to Cytoscape plugins. Nat Methods. 2012; 9:1069–1076. [PubMed: 23132118]
25. Duffy GP, Ahsan T, O'Brien T, et al. Bone marrow-derived mesenchymal stem cells promote angiogenic processes in a time- and dose-dependent manner in vitro. Tissue Eng Part A. 2009; 15:2459–2470. [PubMed: 19327020]

26. Iwase H, Wiegel B, Fehrenbacher G, et al. Comparison between calculation and measured data on secondary neutron energy spectra by heavy ion reactions from different thick targets. Radiat Prot Dosimetry. 2005; 116(pt 2):640–646. [PubMed: 16604717]
27. Kwon HM, Hur SM, Park KY, et al. Multiple paracrine factors secreted by mesenchymal stem cells contribute to angiogenesis. Vasc Pharmacol. 2014; 63:19–28.
28. Chu LH, Rivera CG, Popel AS, et al. Constructing the angiome: A global angiogenesis protein interaction network. Physiol Genom. 2012; 44:915–924.
29. Cline MS, Smoot M, Cerami E, et al. Integration of biological networks and gene expression data using Cytoscape. Nat Protoc. 2007; 2:2366–2382. [PubMed: 17947979]
30. Mi H, Muruganujan A, Casagrande JT, et al. Large-scale gene function analysis with the PANTHER classification system. Nat Protoc. 2013; 8:1551–1566. [PubMed: 23868073]
31. Soccio RE, Breslow JL. Intracellular cholesterol transport. Arterioscler Thromb Vasc Biol. 2004; 24:1150–1160. [PubMed: 15130918]
32. Lev S. Nonvesicular lipid transfer from the endoplasmic reticulum. Cold Spring Harb Perspect Biol. 2012; 4
33. Baenke F, Peck B, Miess H, et al. Hooked on fat: The role of lipid synthesis in cancer metabolism and tumour development. Dis Model Mech. 2013; 6:1353–1363. [PubMed: 24203995]
34. Zhang HC, Liu XB, Huang S, et al. Microvesicles derived from human umbilical cord mesenchymal stem cells stimulated by hypoxia promote angiogenesis both in vitro and in vivo. Stem Cells Dev. 2012; 21:3289–3297. [PubMed: 22839741]
35. Simpson RJ, Kalra H, Mathivanan S. Exo-Carta as a resource for exosomal research. J Extracellular Vesicles. 2012; 1
36. Mathivanan S, Fahner CJ, Reid GE, et al. ExoCarta 2012: Database of exosomal proteins, RNA and lipids. Nucleic Acids Res. 2012; 40:D1241–D1244. Database issue. [PubMed: 21989406]
37. Mathivanan S, Simpson RJ. ExoCarta: A compendium of exosomal proteins and RNA. Proteomics. 2009; 9:4997–5000. [PubMed: 19810033]
38. Bindea G, Mlecnik B, Hackl H, et al. ClueGO: A Cytoscape plug-in to decipher functionally grouped gene ontology and pathway annotation networks. Bioinformatics. 2009; 25:1091–1093. [PubMed: 19237447]
39. Jiang W, Makhlouf F, Schuirmann DJ, et al. A bioequivalence approach for generic narrow therapeutic index drugs: Evaluation of the reference-scaled approach and variability comparison criterion. AAPS J. 2015; 17:891–901. [PubMed: 25840883]
40. Kim HS, Choi DY, Yun SJ, et al. Proteomic analysis of microvesicles derived from human mesenchymal stem cells. J Proteome Res. 2012; 11:839–849. [PubMed: 22148876]
41. Mindaye ST, Ra M, Lo Surdo JL, et al. Global proteomic signature of undifferentiated human bone marrow stromal cells: Evidence for donor-to-donor proteome heterogeneity. Stem Cell Res. 2013; 11:793–805. [PubMed: 23792435]
42. Mindaye ST, Ra M, Lo Surdo J, et al. Improved proteomic profiling of the cell surface of culture-expanded human bone marrow multipotent stromal cells. J Proteomics. 2013; 78:1–14. [PubMed: 23153793]
43. Capoccia BJ, Robson DL, Levac KD, et al. Revascularization of ischemic limbs after transplantation of human bone marrow cells with high aldehyde dehydrogenase activity. Blood. 2009; 113:5340–5351. [PubMed: 19324906]
44. Beckermann BM, Kallifatidis G, Groth A, et al. VEGF expression by mesenchymal stem cells contributes to angiogenesis in pancreatic carcinoma. Br J Cancer. 2008; 99:622–631. [PubMed: 18665180]
45. Deuse T, Peter C, Fedak PW, et al. Hepatocyte growth factor or vascular endothelial growth factor gene transfer maximizes mesenchymal stem cell-based myocardial salvage after acute myocardial infarction. Circulation. 2009; 120(Suppl):S247–S254. [PubMed: 19752375]
46. Fierro FA, Kalomoiris S, Sondergaard CS, et al. Effects on proliferation and differentiation of multipotent bone marrow stromal cells engineered to express growth factors for combined cell and gene therapy. STEM CELLS. 2011; 29:1727–1737. [PubMed: 21898687]
47. Ding W, Knox TR, Tschumper RC, et al. Platelet-derived growth factor (PDGF)-PDGF receptor interaction activates bone marrow-derived mesenchymal stromal cells derived from chronic

lymphocytic leukemia: Implications for an angiogenic switch. Blood. 2010; 116:2984–2993. [PubMed: 20606160]

48. Gianni-Barrera R, Bartolomeo M, Vollmar B, et al. Split for the cure: VEGF, PDGF-BB and intussusception in therapeutic angiogenesis. Biochem Soc Trans. 2014; 42:1637–1642. [PubMed: 25399582]
49. Tabernero J. The role of VEGF and EGFR inhibition: Implications for combining anti-VEGF and anti-EGFR agents. Mol Cancer Res. 2007; 5:203–220. [PubMed: 17374728]
50. Fujioka S, Sclabas GM, Schmidt C, et al. Function of nuclear factor kappaB in pancreatic cancer metastasis. Clin Cancer Res. 2003; 9:346–354. [PubMed: 12538487]
51. Hou Y, Li F, Karin M, et al. Analysis of the IKKbeta/NF-kappaB signaling pathway during embryonic angiogenesis. Dev Dyn. 2008; 237:2926–2935. [PubMed: 18816823]
52. Bronckaers A, Hilkens P, Martens W, et al. Mesenchymal stem/stromal cells as a pharmacological and therapeutic approach to accelerate angiogenesis. Pharmacol Ther. 2014; 143:181–196. [PubMed: 24594234]
53. Lai RC, Arslan F, Lee MM, et al. Exosome secreted by MSC reduces myocardial ischemia/reperfusion injury. Stem Cell Res. 2010; 4:214–222. [PubMed: 20138817]
54. Tan SS, Yin Y, Lee T, et al. Therapeutic MSC exosomes are derived from lipid raft microdomains in the plasma membrane. J Extracell Vesicles. 2013; 2
55. Masson N, Ratcliffe PJ. Hypoxia signaling pathways in cancer metabolism: The importance of co-selecting interconnected physiological pathways. Cancer Metab. 2014; 2:3. [PubMed: 24491179]
56. Li T, Yan Y, Wang B, et al. Exosomes derived from human umbilical cord mesenchymal stem cells alleviate liver fibrosis. Stem Cells Dev. 2013; 22:845–854. [PubMed: 23002959]
57. Katsuda T, Tsuchiya R, Kosaka N, et al. Human adipose tissue-derived mesenchymal stem cells secrete functional neprilysin-bound exosomes. Sci Rep. 2013; 3:1197. [PubMed: 23378928]
58. Lin SS, Zhu B, Guo ZK, et al. Bone marrow mesenchymal stem cell-derived microvesicles protect rat pheochromocytoma PC12 cells from glutamate-induced injury via a PI3K/Akt dependent pathway. Neurochem Res. 2014; 39:922–931. [PubMed: 24706151]
59. Bruno S, Grange C, Deregibus MC, et al. Mesenchymal stem cell-derived microvesicles protect against acute tubular injury. J Am Soc Nephrol. 2009; 20:1053–1067. [PubMed: 19389847]
60. Xin H, Li Y, Liu Z, et al. MiR-133b promotes neural plasticity and functional recovery after treatment of stroke with multipotent mesenchymal stromal cells in rats via transfer of exosome-enriched extracellular particles. Stem Cells. 2013; 31:2737–2746. [PubMed: 23630198]

Significance Statement

The clinical relevance of MSC-based therapeutics has been firmly established ahead of the field's understanding of how their beneficial effects are mediated. Interestingly, MSC-derived exosomes are gaining momentum in the field as a putative surrogate to MSC-based therapeutics with a stronger safety profile. Indeed the first patient has already been successfully treated with MSC-exosomes for GvHD. Our study is the first to comprehensively characterize the functional protein contents of MSC and their exosomes thereby shedding light on how they mediate their beneficial effects in the clinic and may lead to more efficacious precision-engineered MSC-based therapeutics.

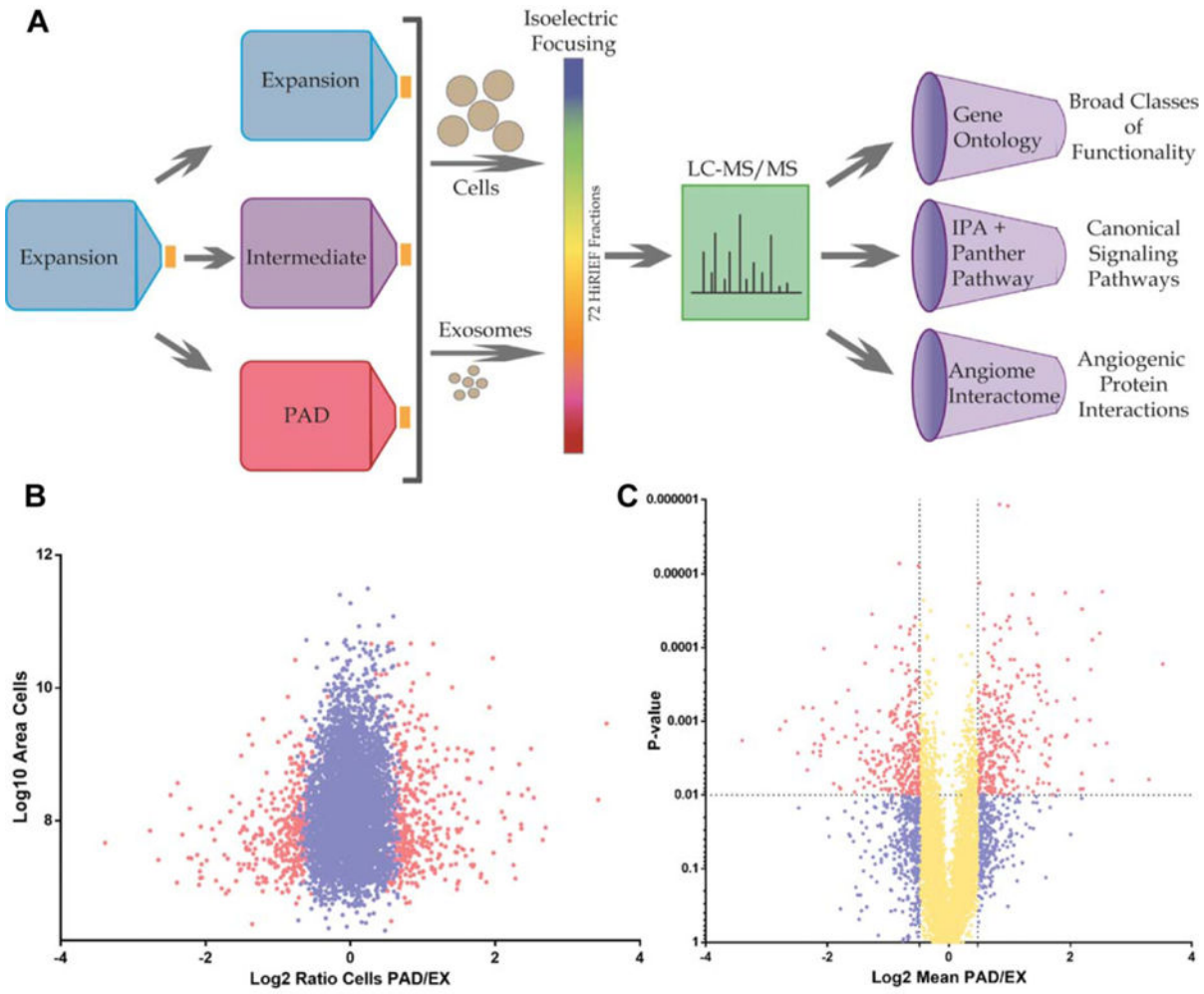

Figure 1.

Experimental design workflow and ratio distribution of mesenchymal stem cell (MSC) proteomics. **(A)**: Schematic representation of proteomics workflow. MSCs were isolated from human bone marrow and expanded to passage 6 using EX conditions. Cells were then washed three times with phosphate buffered saline and switched to either EX, IC, or PAD-like (PAD) conditions for 40 hours. Cells or exosomes were then lysed, trypsinized, and ran on high-resolution isoelectric focusing strips which were divided into 72 individual fractions and ran on LC-MS/MS. Identified proteins were analyzed using three different types of analysis software: gene ontology, canonical signaling pathways, and network analysis of the angiome interactome. ClueGO gene ontology analysis was used to characterize enrichment for proteins based on their functionalities. Panther and Ingenuity pathway analysis were used to characterize enrichment for proteins of specific canonical signaling pathways. CytoScape network analysis of the angiome interactome was used to visualize the physical interactions of known angiogenesis-mediating proteins (angiome) with proteins for which there is experimental evidence of physical interaction. **(B)**: Plot of PAD/EX ratios (Log2, fold change) versus area (Log10, abundance) of MSC proteins; red dots represent significantly differentially expressed proteins (FDR1% [false discovery rate]), blue dots represent all nonsignificantly differentially expressed proteins. **(C)**: PAD/EX ratios (Log2, fold change)

versus *p* value; yellow dots represent differentially expressed proteins with mean fold changes < ±0.5 Log2, red dots represent > ±0.5 Log2 mean fold change with *p* value < .01 and blue dots with a *p* value of >.01. Abbreviations: EX, expansion condition; LC-MS/MS, liquid chromatography tandem mass spectrometry; PAD, peripheral arterial disease.

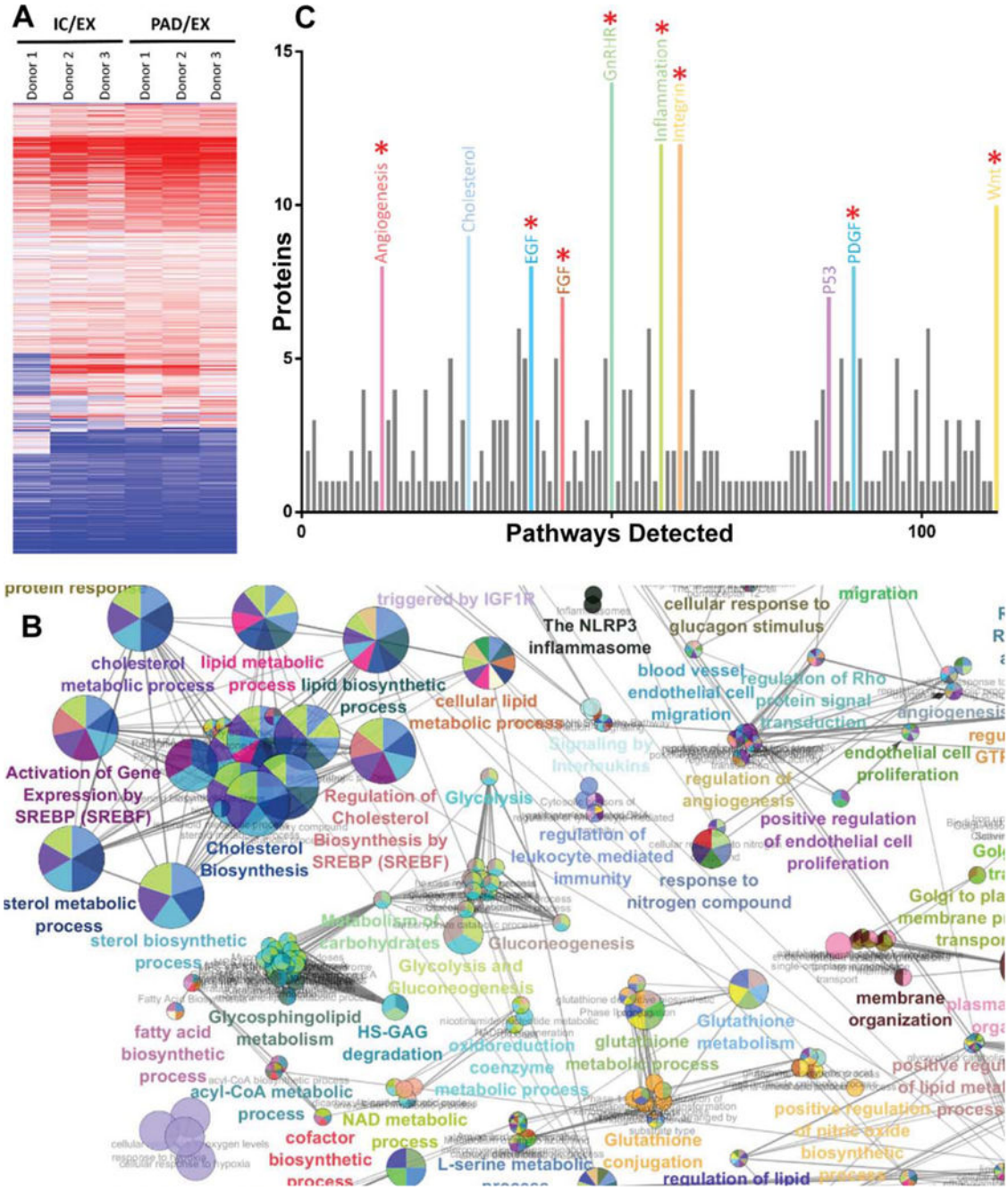

Figure 2.

Analysis of high-resolution isoelectric focusing coupled liquid chromatography tandem mass spectrometry proteomics data from IC and PAD conditions compared to control condition EX. **(A)**: Heatmap of mesenchymal stem cell (MSC) cluster analysis of differentially regulated proteins in IC and PAD conditions as compared to EX. **(B)**: ClueGO gene ontology analysis of proteins upregulated in PAD MSCs shows enrichment for cholesterol biosynthesis, lipid biosynthesis, angiogenesis, and glycolysis associated proteins. **(C)**: Panther pathway analysis of proteins upregulated in MSCs under PAD-like conditions show abundance of canonical angiogenesis related pathway proteins: epidermal growth

factor, fibroblast growth factor, and platelet derived growth factor (red asterisk indicate angiogenesis associated pathways). Analysis of three different donors for each condition. For differential expression *t* tests with multiple testing correction with an false discovery rate of 1% was used. Circles are color coded according to their associated functionality. Number of circles and larger diameter of circles indicate greater over representation. Abbreviations: EX, expansion condition; IC, intermediate condition; PAD, peripheral arterial disease.

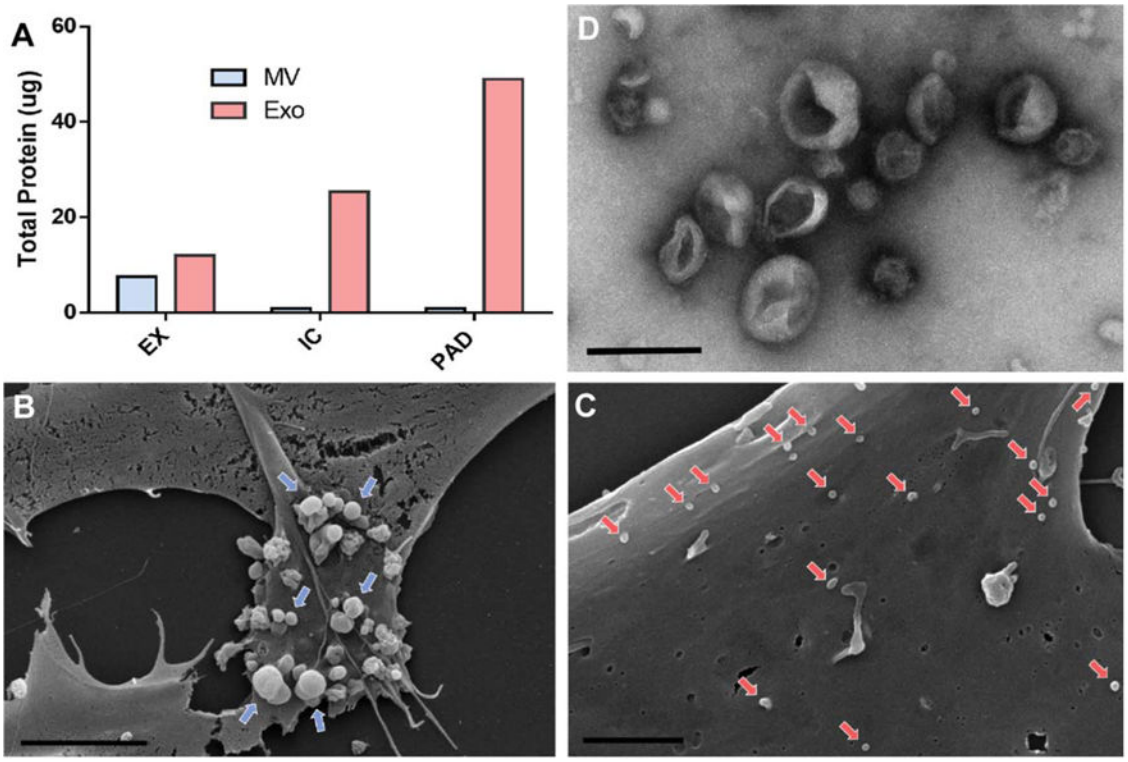

Figure 3.

Mesenchymal stem cells (MSCs) increase secretion of exosomes upon exposure to PAD-like conditions. **(A)**: Quantification of total protein content of vesicles derived from MSC under EX, IC, and PAD culture conditions using DC assay. **(B)**: Scanning electron micrograph of MSCs cultured in EX culture conditions indicating microvesicle release (blue arrows) from the cell surface (scale bar = 5 μm, × 5k). **(C)**: Scanning electron micrograph of MSCs cultured under PAD conditions (scale bar 2 μm, × 10k) indicating exosome adhesion to cell surface (red arrows). **(D)**: Transmission electron micrograph of MSC derived exosomes with 2% uranyl acetate negative staining (scale bar 200 nm, × 25k). Abbreviations: EX, expansion condition; Exo, exosomes; IC, intermediate condition; MV, microvesicle; PAD, peripheral arterial disease.

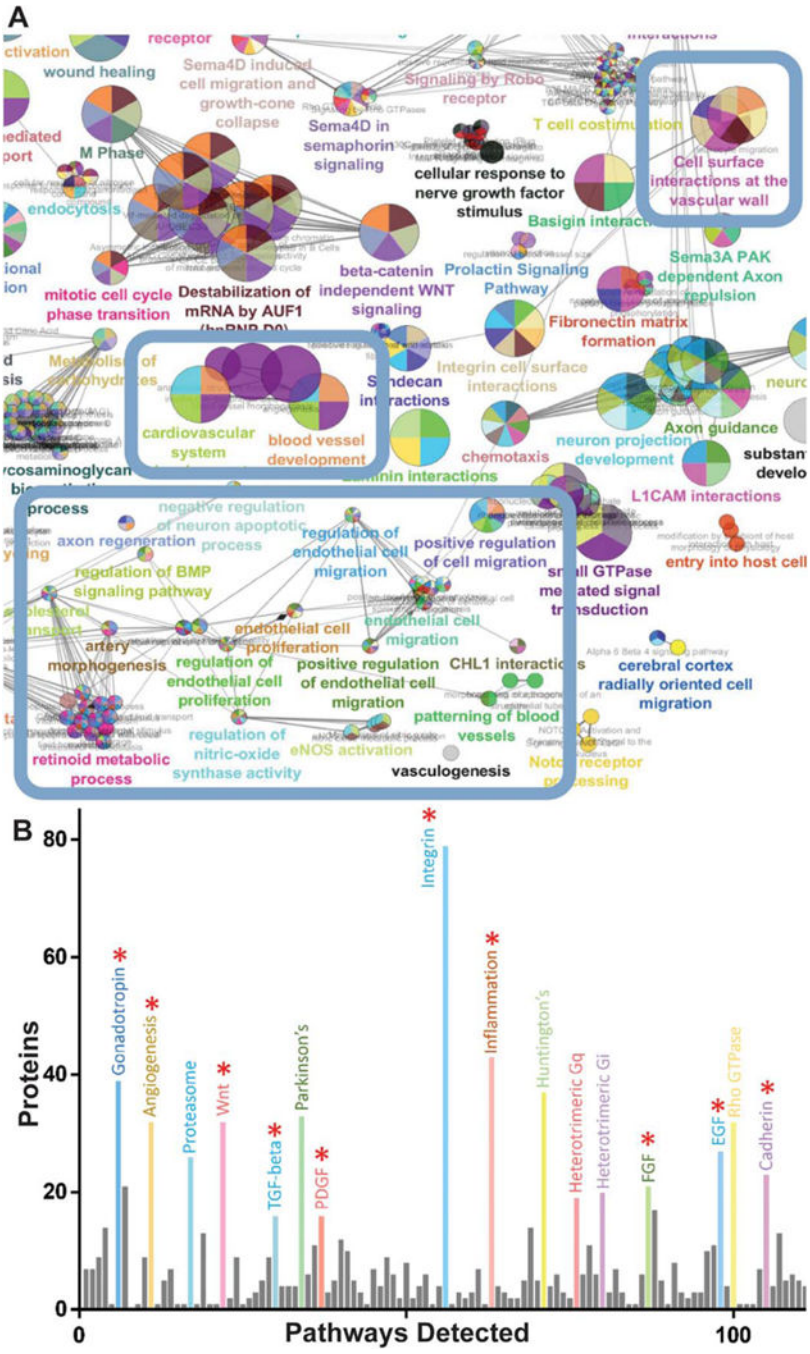

Figure 4.

Analysis of high-resolution isoelectric focusing coupled liquid chromatography tandem mass spectrometry proteomics data of mesenchymal stem cell (MSC) exosomes comparing peripheral arterial disease (PAD) to intermediate condition (IC). **(A)**: ClueGO network analysis of 400 most abundant proteins in PAD exosomes shows enrichment for effector proteins (blue boxes). **(B)**: Panther pathway analysis of PAD exosomes shows abundance of angiogenesis related pathway proteins: epidermal growth factor receptor, fibroblast growth factor, and platelet derived growth factor pathway associated proteins (red asterisk indicate

angiogenesis associated pathways). Analysis of three different donors for each condition. For differential expression *t* tests with multiple testing correction with an false discovery rate of 1% was used. Circles are color coded according to their associated functionality. Number of circles and larger diameter of circles indicate greater over representation.

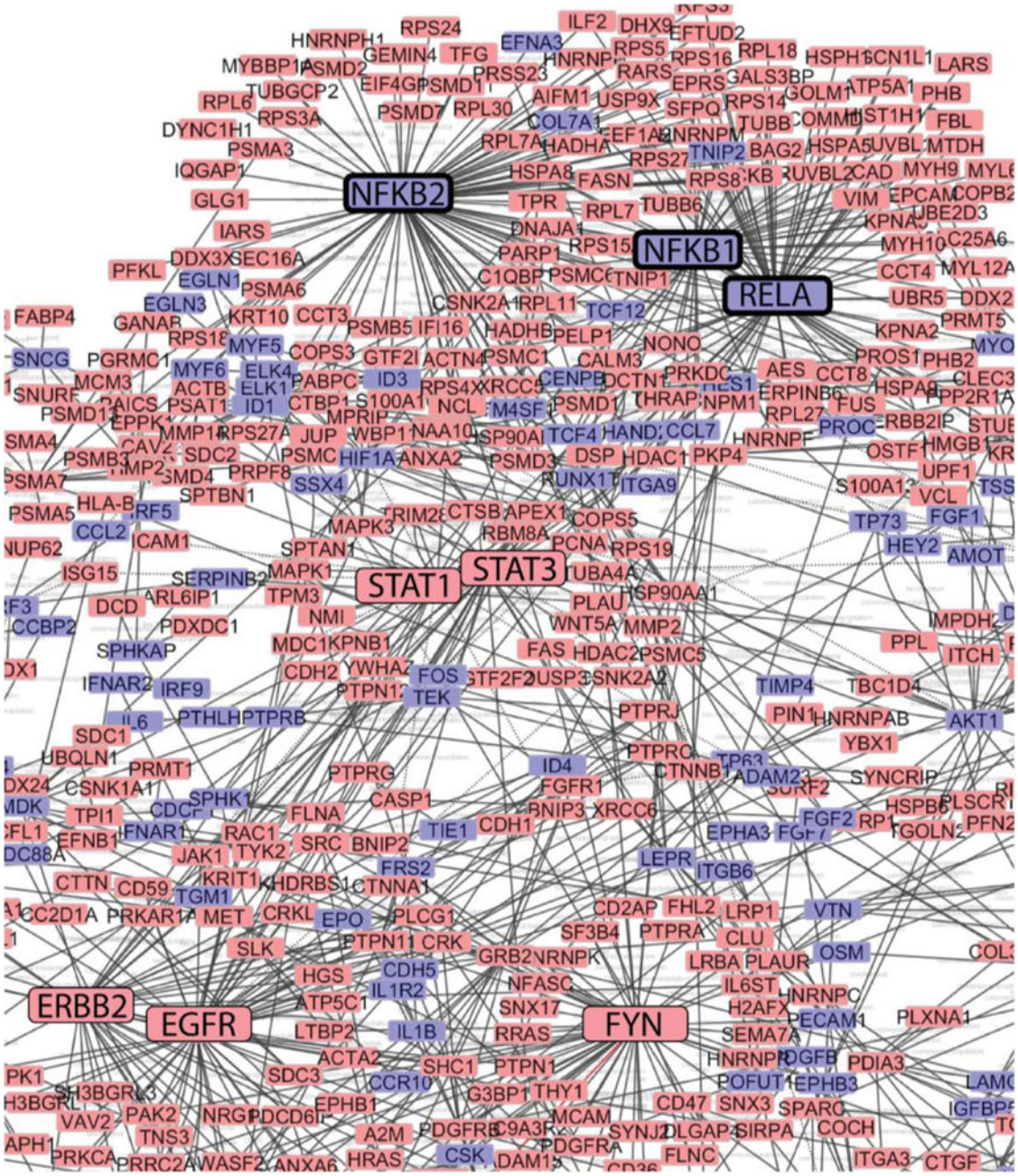

Figure 5.

Network analysis of mesenchymal stem cell (MSC) exosome angiogenesis interactome. Network analysis using CytoScape of the MSC exosome angiogenesis interactome reveals clustering around nodes involved in nuclear factor kappaB signaling (emboldened boxes). Red boxes indicate presence of angiome interacting proteins in MSC exosomes, blue boxes indicate absence of these network proteins in MSC exosomes. Boxes of major clustering nodes of known effectors were enlarged for clarity. Edges connecting boxes indicates experimental evidence of physical contact (e.g., coimmunopreciptitation, yeast-2-hybrid).

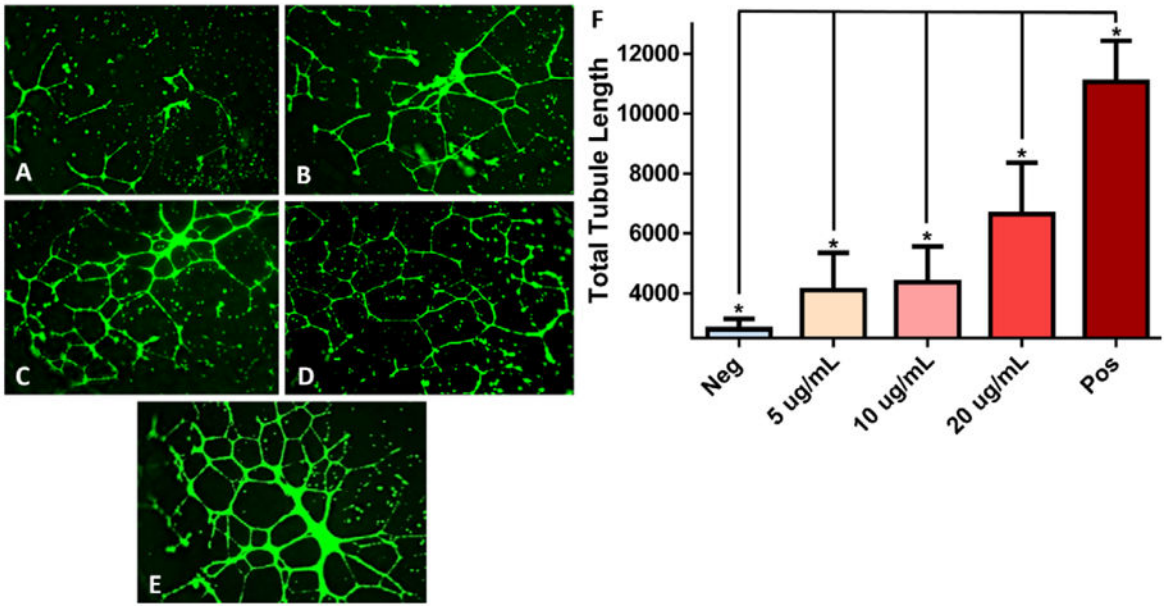

Figure 6.

Mesenchymal stem cell (MSC) exosome-induced in vitro tubule formation of human umbilical cord vein endothelial cells. **(A)**: Basal media (Neg), **(B)** 5 μg/mL, **(C)** 10 μg/mL, **(D)** 20 μg/mL of MSC exosomes in basal media, **(E)** EndoGRO media positive control (Pos). Stained with Calcein AM and imaged at 14 hours poststimulation with × 4 objective. **(F)**: Quantification of total segment length of tubule formation analyzed using ImageJ's Angiogenesis plugin. EndoGRO positive control media contains 2% fetal bovine serum, epidermal growth factor 5 ng/mL and heparin sulfate 0.75 U/mL. (*) Indicates a p value < . 05 using ANOVA, LSD post hoc analysis (n = 12).

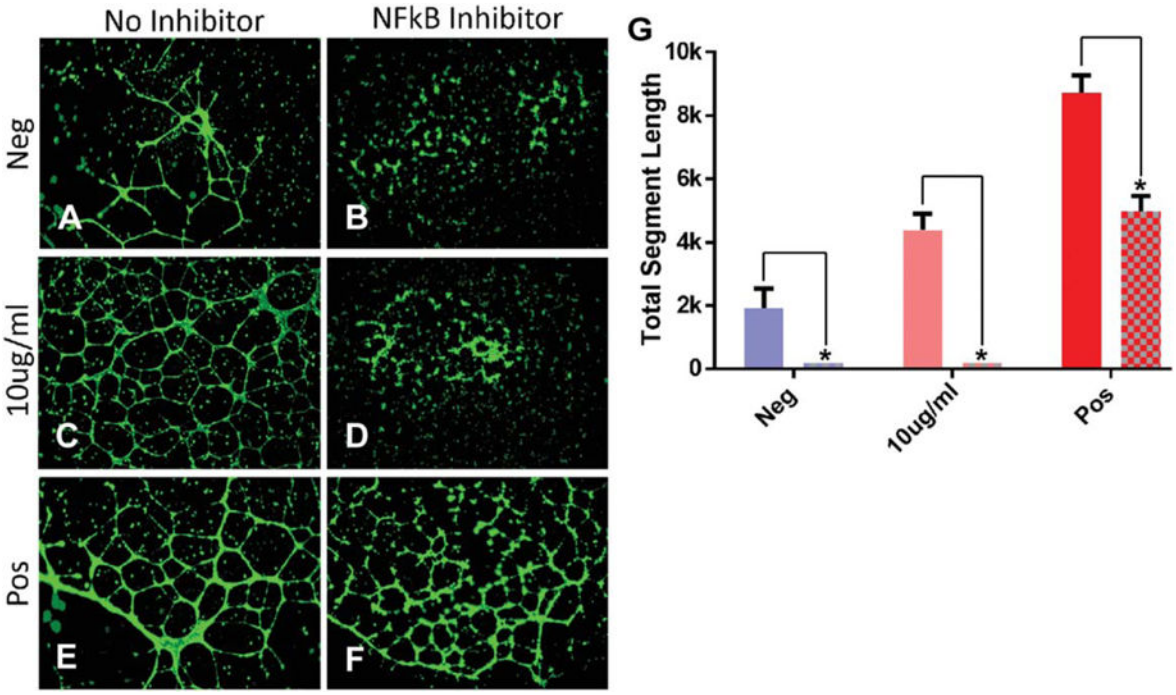

Figure 7.

NFkB inhibition abrogates mesenchymal stem cell (MSC) exosome-mediated tubule formation in human umbilical cord vein endothelial cells (HUVECs) in vitro. **(A)** Basal media, **(B)** basal media + NFkB inhibitor, **(C)** 10 μg/mL, **(D)** 10 μg/mL + NFkB inhibitor, **(E)** EndoGRO media, **(F)** EndoGRO media + NFkB inhibitor. HUVECs stained with Calcein AM and imaged 14 hours poststimulation with a ×4 objective. **(G)**: Quantification of total segment length of tubule formation using ImageJ's Angiogenesis plugin. EndoGRO media contains 2% fetal bovine serum, epidermal growth factor 5 ng/mL, and heparin sulfate 0.75 U/mL. (*) Indicates a p value < .01 using ANOVA, LSD post hoc analysis ($n = 6$). Abbreviation: NFkB, nuclear factor kappaB.